Quantum walker as a probe for its coin parameter

Shivani Singh[*] and C. M. Chandrashekar[†]
The Institute of Mathematical Sciences, CIT campus, Taramani, Chennai 600113, India
and Homi Bhabha National Institute, Training School Complex, Anushakti Nagar, Mumbai 400094, India

Matteo G. A. Paris[‡]
Quantum Technology Lab, Dipartimento di Fisica "Aldo Pontremoli," Università degli Studi di Milano, I-20133 Milano, Italy

(Received 8 January 2019; revised manuscript received 25 March 2019; published 20 May 2019)

In discrete-time quantum walk (DTQW) the walker's coin space entangles with the position space after the very first step of the evolution. This phenomenon may be exploited to obtain the value of the coin parameter θ by performing measurements on the sole position space of the walker. In this paper, we evaluate the ultimate quantum limits to precision for this class of estimation protocols and use this result to assess measurement schemes having limited access to the position space of the walker in one dimension. We find that the quantum Fisher information (QFI) of the walker's position space $H_w(\theta)$ increases with θ and with time, which, in turn, may be seen as a metrological resource. We also find a difference in the QFI of *bounded* and *unbounded* DTQWs and provide an interpretation of the different behaviors in terms of interference in the position space. Finally, we compare $H_w(\theta)$ to the full QFI $H_f(\theta)$, i.e., the QFI of the walkers position plus coin state, and find that their ratio is dependent on θ, but saturates to a constant value, meaning that the walker may probe its coin parameter quite faithfully.

DOI: 10.1103/PhysRevA.99.052117

I. INTRODUCTION

Quantum walk is the quantum analog of random walk which, in turn, provides a relevant model for the dynamics of various classical systems [1,2]. Quantum superposition and interference strongly affect the dynamics of a quantum walker and this leads to a quadratically faster spread in position space when compared to a classical walker [3–9]. This feature made quantum walks a powerful tool in quantum computation [10–14], as well as to model the dynamics of different quantum systems, such as energy transport in photosynthesis [15,16], quantum percolation [17,18], and graph isomorphism [19].

As in classical random walk, quantum walk has also been developed in two forms, continuous-time and discrete-time quantum walk (DTQW). Both the variants have been shown to efficiently implement any quantum computational task [19,20]. Continuous-time quantum walk is defined only on position Hilbert space, whereas discrete-time quantum walk is defined on a joint position and *coin* Hilbert space, thus providing an additional degree of freedom to control the dynamics. Upon tuning the different parameters of the evolution operators of DTQW, one may control and engineer the dynamics in order to *simulate* various quantum phenomena such as localization [21–23], topological phase [24,25], neutrino oscillation [26,27], and relativistic quantum dynamics [28–34]. Quantum walks have been experimentally implemented in various physical systems such as NMR [35], photonics [36–39], cold atoms [40], and trapped ions [41,42].

Evolution in discrete-time quantum walk is defined by unitary *coin operation* followed by a unitary *position shift operator*. The shift operator evolves the walker in a superposition of the position states, with amplitudes governed by the operation on coin Hilbert space. The most general unitary coin operator in one dimension has three independent parameters [43] and provides an ample control over the dynamics, but already one- and two-parameter coins are extremely useful in simulating various physical systems in one dimension. For example, different combinations of evolution parameters in split-step DTQW describe topological phases [24,25] and neutrino oscillation [26,27]. Indeed, coin parameters play a relevant role in the evolution of the state of the walker in the position space and, in turn, in controlling and engineering DTQWs. In this framework, a precise knowledge of the coin parameters is crucial information for quantum simulations and for further development in the use of quantum walks to model realistic quantum dynamics.

In the past, it has been determined that one coin parameter determines the group velocity of the walker's spread in position space [44]. Therefore, by studying the standard deviation or group velocity of DTQW with one coin parameter, one can determine the value of parameter θ for unbounded DTQW. But the same does not hold for bounded or multiparameter coin QW. Fisher information (FI) measures the amount of information that can be obtained about the unknown parameters in the system by performing measurement on the system, individually. Therefore, it can be used to obtain information of all the coin parameters when the coin operator is a general SU(2) operator with three-parameters coin operation,

[*]shivanis@imsc.res.in
[†]chandru@imsc.res.in
[‡]matteo.paris@fisica.unimi.it

multicoin operation, or the bounded case. Here, we first develop a technique to calculate Fisher information in DTQW using a one-parameter coin operator, and then extend to two-coin quantum walk. In this paper, we first consider a coin operator with one parameter θ and address the evolution of bounded and unbounded DTQWs in one dimension. Our aim is to design optimal estimation techniques for the coin parameter based on measurements performed on the sole position space of the walker. Our approach belongs to the class of protocols usually referred to as quantum probing [45–56], which proved useful to precisely extract information upon exploiting the inherent sensitivity of quantum systems to external perturbations.

We use the FI to quantify the information about a parameter θ which may be extracted by performing a given measurement on a quantum system. In particular, we consider the FI $F_w(\theta)$ of the generic measurement performed on the walker's position degree of freedom. The maximum of $F_w(\theta)$ over all the possible measurements is the so-called quantum Fisher information $H_w(\theta)$ (QFI), which quantifies the ultimate quantum bound to the extractable information, i.e., the overall information encoded onto the state of the system. We also evaluate the full QFI $H_f(\theta)$, i.e., the QFI of the position plus coin state, in order to assess the overall performances of measurements on the sole position space of the walker, compared to measurements having access to the full quantum state. Our results show that the walker QFI $H_w(\theta)$ increases as t^2, as it happens for the full QFI $H_f(\theta)$, meaning that the walker is a good probe for its coin operation parameter θ. Additionally, the walker's position QFI $H_w(\theta)$ increases with θ and then decreases slowly up to $\pi/2$ (and then mimics in the mirrored way, due to symmetry in the coin operator up to π). Finally, we analyze in some detail the performances of position measurement on the walker; i.e., we assess how much information on the coin parameter may be extracted by looking at the probability distribution of the walker at a given time. We also present QFI in position space for split-step quantum walk, where we have two coin parameters; we can see that QFI $H_w(\theta)$ helps us to estimate the coin parameters.

The paper is structured as follows. In Sec. II, we describe bounded and unbounded DTQWs and the evolution operators governing their dynamics. In Sec. III we review quantum estimation theory, describe a method to numerically calculate the walker's quantum Fisher information in DTQWs, and illustrate the main results of our analysis. Section IV closes the paper with some concluding remarks.

II. EVOLUTION IN DISCRETE-TIME QUANTUM WALK

DTQW of a single walker on a one-dimensional lattice is defined on the Hilbert space $\mathcal{H} = \mathcal{H}_c \otimes \mathcal{H}_p$ where $\mathcal{H}_p$ and $\mathcal{H}_c$ are the position and the coin Hilbert spaces of the walker, respectively. The basis states of the coin Hilbert space are $\{|\uparrow\rangle, \langle\downarrow|\}$, which may be seen as the internal states of the walker. The position Hilbert space is spanned by the basis $|x\rangle$ where $x \in \mathbb{Z}$. The initial state of the system is usually taken in the form

$$|\Psi_{\text{in}}\rangle = \alpha\,|\uparrow\rangle + \beta\,|\downarrow\rangle \otimes |x=0\rangle\,, \quad |\alpha|^2 + |\beta|^2 = 1. \tag{1}$$

Here α and β are the amplitudes of the states $|\uparrow\rangle$ and $|\downarrow\rangle$, respectively. The evolution operator for discrete-time quantum walk is defined by the action of unitary quantum coin operation followed by a position shift operator. The single-parameter coin operator is given by

$$C_\theta = \begin{pmatrix} \cos\theta & -i\sin\theta \\ -i\sin\theta & \cos\theta \end{pmatrix} \otimes \sum_x |x\rangle\langle x| \tag{2}$$

whereas the shift operator S is defined with reference to the size of the region accessible by the walker. *Unbounded* DTQWs are defined on a position Hilbert space of infinite size. The walker has no boundary condition on probability amplitude, and the position shift operator is given by

$$S_x = \sum_x |\uparrow\rangle\langle\uparrow| \otimes |x-1\rangle\langle x| + |\downarrow\rangle\langle\downarrow| \otimes |x+1\rangle\langle x|\,. \tag{3}$$

In Fig. 1 we show the probability distribution after 200 time steps for an unbounded DTQW using different values of coin parameter θ. The smaller the value of θ, the larger the spread of the probability distribution. *Bounded* DTQWs evolve instead on finite position Hilbert spaces, characterized by a finite number of sites and boundary conditions. In turn, the position shift operator is bounded between $[-a, a]$ with boundary condition $|\Psi_{a+1}\rangle = |\Psi_{-a-1}\rangle = 0$, where $a \in \mathbb{Z}$. In formula,

$$S_x = |\downarrow\rangle\langle\uparrow| \otimes |-a\rangle\langle -a| + \sum_{x=-a+1}^{a} |\uparrow\rangle\langle\uparrow| \otimes |x-1\rangle\langle x| + \sum_{x=-a}^{a-1} |\downarrow\rangle\langle\downarrow| \otimes |x+1\rangle\langle x| + |\uparrow\rangle\langle\downarrow| \otimes |a\rangle\langle a|\,. \tag{4}$$

The insets of Fig. 1 show the probability distribution after 200 time steps for a bounded DTQW and for different values of θ. The position space is bounded between –50 and 50. In this case the shape of the probability distribution arises from the interplay of the coin operator and the bounded nature of the position space, and the spread cannot be simply characterized as a function of θ, as it was for unbounded walk.

In general, after t steps in the evolution, the overall state of the particle will be of the form

$$|\Psi_t\rangle = (S_x\,C_\theta)^t\,|\Psi_{\text{in}}\rangle = \sum_x (\mathcal{A}_{x,t}\,|\uparrow\rangle + \mathcal{B}_{x,t}\,|\downarrow\rangle) \otimes |x\rangle, \tag{5}$$

where $\mathcal{A}_{x,t}$ and $\mathcal{B}_{x,t}$ are the amplitudes of the states $|\uparrow\rangle$ and $|\downarrow\rangle$ at position x at time t, respectively. The $\mathcal{A}$ and $\mathcal{B}$ coefficients are in turn linked by the iterative relations

$$\begin{pmatrix} \mathcal{A}_{x,t} \\ \mathcal{B}_{x,t} \end{pmatrix} = \begin{pmatrix} \cos\theta & -i\sin\theta \\ 0 & 0 \end{pmatrix} \begin{pmatrix} \mathcal{A}_{x+1,t-1} \\ \mathcal{B}_{x+1,t} \end{pmatrix} + \begin{pmatrix} 0 & 0 \\ -i\sin\theta & \cos\theta \end{pmatrix} \begin{pmatrix} \mathcal{A}_{x-1,t-1} \\ \mathcal{B}_{x-1,t-1} \end{pmatrix} \tag{6}$$

for both unbounded and bounded discrete-time quantum walk (when the walker is away from the boundary). Therefore, the probability of finding the particle at position x and at time t is given by

$$P(x,t) = |\mathcal{A}_{x,t}|^2 + |\mathcal{B}_{x,t}|^2. \tag{7}$$

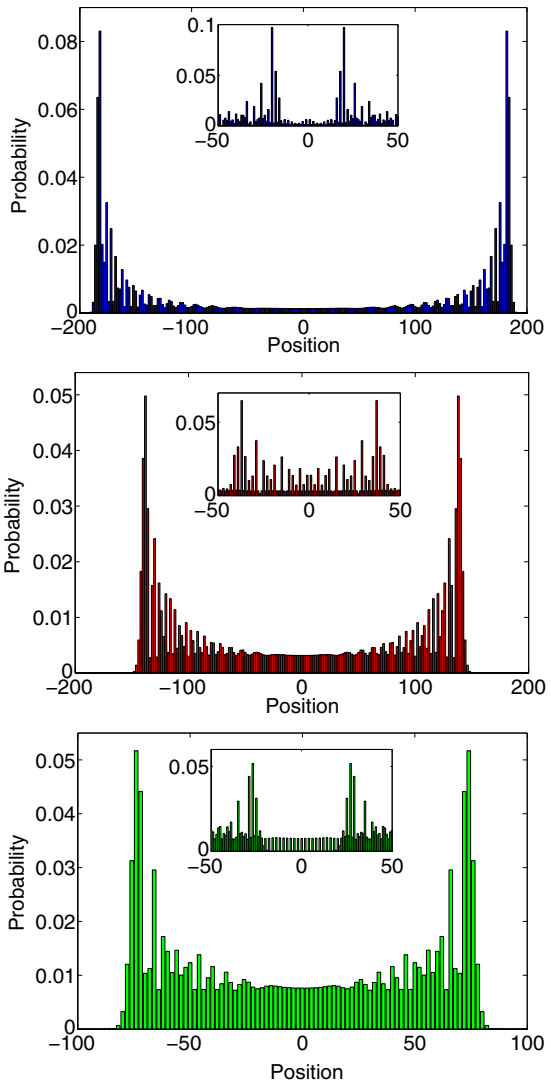

FIG. 1. Probability distribution of unbounded DTQW in one dimension after 200 time steps for different values of θ. The insets show the corresponding distributions for a DTQW bounded in the region $[-50, 50]$. In both cases the initial state of the system has been set to $\frac{1}{\sqrt{2}}(|\uparrow\rangle + |\downarrow\rangle) \otimes |x = 0\rangle \equiv |+\rangle \otimes |0\rangle$.

III. QUANTUM ESTIMATION IN DISCRETE-TIME QUANTUM WALK

The Fisher information provides a measure of the amount of information that the observable X carries about a parameter ξ, usually a quantity of interest, influencing its probability distribution $p(x|\xi)$ [57]. In more detail, the Fisher information $F(\xi)$ of a conditional distribution $p(x|\xi)$ is given by

$$F(\xi) = \int dx\, p(x|\xi) \left[\frac{\partial \ln p(x|\xi)}{\partial \xi}\right]^2, \tag{8}$$

where, as mentioned above, $p(x|\xi)$ is the probability of obtaining the outcome x from the measurement of X when the true value of the parameter is ξ. If the available data for the observable X are coming from M repeated independent measurements of X, i.e., $\mathbf{x} = (x_1, x_2, \ldots, x_M)$, then the overall probability of the sample (the likelihood) is $p(\mathbf{x}|\xi) = \Pi_{k=1}^{M} p(x_k|\xi)$, which depends upon the parameter ξ to be estimated. An *estimator* $\hat{\xi}(\mathbf{x})$ is a function of the data sample, which provides an estimate of the value of the parameter ξ. Since data fluctuate, the value of the estimator fluctuates as well. The variance $\mathrm{Var}_\xi \hat{\xi}$ of $\hat{\xi}$ provides a measure of the precision of the overall estimation procedure (i.e., the measurement of X followed by the data processing $\hat{\xi}$). The Cramer-Rao theorem states that the Fisher information poses a bound of the variance of $\hat{\xi}$:

$$\mathrm{Var}_\xi \hat{\xi} \geqslant \frac{1}{MF(\xi)}. \tag{9}$$

The larger the value of $F(\xi)$, the greater the amount of information about ξ that *may* be, *in principle*, extracted from the measurement of X. The actual information on ξ obtained from measuring X instead depends on the estimator. An estimator saturating the Cramer-Rao bound of Eq. (9) is said to be *efficient*. In the following, we assume that an efficient estimator is available and compare the performances of different measurements in terms of their Fisher information.

Let us now move to quantum measurements: According to Born's rule the conditional distribution $p(x|\xi)$ may be written as $p(x|\xi) = \mathrm{Tr}[\Pi_x \rho_\xi]$, where Π_x is the probability operator-valued measure of the measured quantity X, and the dependence on ξ is encoded onto the preparation of the system undergoing the measurement, i.e., the density ρ_ξ. An upper bound on the Fisher information of *any* quantum measurement may be obtained by introducing the symmetric logarithmic derivative (SLD) L_ξ, which satisfies the relation

$$\tfrac{1}{2}(L_\xi \rho_\xi + \rho_\xi L_\xi) = \frac{\partial \rho_\xi}{\partial \xi}. \tag{10}$$

Then, since $\partial_\xi p(x|\xi) = \mathrm{Tr}[\partial_\xi \rho_\xi \Pi_x] = \mathrm{Re}(\mathrm{Tr}[\rho_\xi \Pi_x L_\xi])$, the Fisher information may be rewritten in terms of L_ξ and an upper bound on Fisher information, usually referred to as quantum Fisher information, may be found:

$$F(\xi) \leqslant H(\xi) \equiv \mathrm{Tr}\big[\rho_\xi L_\xi^2\big], \tag{11}$$

where L_ξ is given in Eq. (10). For a pure state, $\rho_\xi^2 = \rho_\xi$ and therefore $\partial_\xi \rho_\xi = (\partial_\xi \rho_\xi)\rho_\xi + \rho_\xi(\partial_\xi \rho_\xi)$ implies $L_\xi = 2\partial_\xi \rho_\xi$. Hence, encoding $\rho_\xi = |\psi_\xi\rangle\langle\psi_\xi|$, the SLD reduces to $L_\xi = 2\partial_\xi \rho_\xi$.

A. The full QFI $H_f(\theta)$ in discrete-time quantum walk

The density matrix of the full (coin plus position) state in the complete Hilbert space $\mathcal{H} = \mathcal{H}_c \otimes \mathcal{H}_w$ at time t is given by

$$\rho_\theta = |\Psi_\theta\rangle\langle\Psi_\theta| \equiv \begin{pmatrix} |\psi_\theta^\uparrow\rangle \\ |\psi_\theta^\downarrow\rangle \end{pmatrix} \begin{pmatrix} \langle\psi_\theta^\uparrow| \\ \langle\psi_\theta^\downarrow| \end{pmatrix}^T \tag{12}$$

where the size of the vector $|\psi_\theta^\uparrow\rangle$ and $|\psi_\theta^\downarrow\rangle$ is equal to the dimension of the walker's position Hilbert space $\mathcal{H}_w$ and the dimension of ρ_θ is $2N$ where N is the dimension of $\mathcal{H}_w$. This

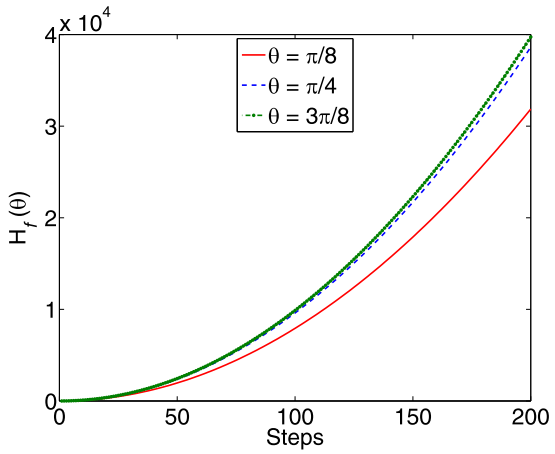

FIG. 2. The full QFI $H_f(\theta)$ as a function of time for different values of θ. The initial state of the system is $|+\rangle \otimes |0\rangle$. The full QFI $H_f(\theta)$ is the same for bounded and unbounded DTQWs.

implies that $\partial_\theta \rho_\theta$ may be written as

$$\begin{aligned}\partial_\theta \rho_\theta &= |\partial_\theta \Psi_\theta\rangle \langle \Psi_\theta| + |\Psi_\theta\rangle \langle \partial_\theta \Psi_\theta| \\ &= \begin{pmatrix} |\partial_\theta \psi_\theta^\uparrow\rangle \\ |\partial_\theta \psi_\theta^\downarrow\rangle \end{pmatrix} \begin{pmatrix} \langle \psi_\theta^\uparrow| \\ \langle \psi_\theta^\downarrow| \end{pmatrix}^T + \begin{pmatrix} |\psi_\theta^\uparrow\rangle \\ |\psi_\theta^\downarrow\rangle \end{pmatrix} \begin{pmatrix} \langle \partial_\theta \psi_\theta^\uparrow| \\ \langle \partial_\theta \psi_\theta^\downarrow| \end{pmatrix}^T \end{aligned} \tag{13}$$

and $|\partial_\theta \Psi_\theta\rangle$ at time t is given by

$$|\partial_\theta \Psi_\theta(t)\rangle = S_x C_\theta |\partial_\theta \Psi_\theta(t-1)\rangle + S_x(\partial_\theta C_\theta)|\Psi_\theta(t-1)\rangle \tag{14}$$

where

$$\partial_\theta C_\theta = \begin{pmatrix} -\sin\theta & -i\cos\theta \\ -i\cos\theta & -\sin\theta \end{pmatrix} \otimes \sum_x |x\rangle \langle x| . \tag{15}$$

As a consequence, if at a given time t we have the amplitude $\Psi_x = (\psi_x^\uparrow; \psi_x^\downarrow) = (\mathcal{A}_x, \mathcal{B}_x)$, then the iterative form for $|\partial_\theta \Psi_\theta(t)\rangle$ is given by

$$\begin{aligned}\begin{pmatrix} \partial_\theta \mathcal{A}_{t,x} \\ \partial_\theta \mathcal{B}_{t,x} \end{pmatrix} &= \begin{pmatrix} \cos(\theta) & -i\sin(\theta) \\ 0 & 0 \end{pmatrix} \begin{pmatrix} \partial_\theta \mathcal{A}_{t-1,x+1} \\ \partial_\theta \mathcal{B}_{t-1,x+1} \end{pmatrix} \\ &+ \begin{pmatrix} 0 & 0 \\ -i\sin\theta & \cos\theta \end{pmatrix} \begin{pmatrix} \partial_\theta \mathcal{A}_{t-1,x-1} \\ \partial_\theta \mathcal{B}_{t-1,x-1} \end{pmatrix} \\ &+ \begin{pmatrix} -\sin\theta & -i\cos\theta \\ 0 & 0 \end{pmatrix} \begin{pmatrix} \mathcal{A}_{t-1,x+1} \\ \mathcal{B}_{t-1,x+1} \end{pmatrix} \\ &+ \begin{pmatrix} 0 & 0 \\ -i\cos\theta & -\sin\theta \end{pmatrix} \begin{pmatrix} \mathcal{A}_{t-1,x-1} \\ \mathcal{B}_{t-1,x-1} \end{pmatrix} . \end{aligned} \tag{16}$$

Upon substituting Eqs. (12) and (13) in Eq. (11) we obtain the quantum Fisher information $H_f(\theta)$ in the complete Hilbert space $\mathcal{H} = \mathcal{H}_c \otimes \mathcal{H}_w$, i.e., the information extractable from the full quantum state of the walker's position plus coin system. In Fig. 2 we show $H_f(\theta)$ for unbounded and bounded DTQWs after 200 time steps. The full QFI $H_f(\theta)$ increases as t^2 with time and it is the same for bounded and unbounded DTQWs.

B. The walker's position space QFI $H_w(\theta)$ in discrete-time quantum walk

The density matrix of the sole position space of the walker is obtained by tracing out the coin degree of freedom from Eq. (12). We have

$$\rho_w(\theta) = |\psi_\theta^\uparrow\rangle \langle \psi_\theta^\uparrow| + |\psi_\theta^\downarrow\rangle \langle \psi_\theta^\downarrow| \tag{17}$$

and, in turn,

$$\begin{aligned}\partial_\theta \rho_w(\theta) = &|\partial_\theta \psi_\theta^\uparrow\rangle \langle \psi_\theta^\uparrow| + |\psi_\theta^\uparrow\rangle \langle \partial_\theta \psi_\theta^\uparrow| \\ &+ |\partial_\theta \psi_\theta^\downarrow\rangle \langle \psi_\theta^\downarrow| + |\psi_\theta^\downarrow\rangle \langle \partial_\theta \psi_\theta^\downarrow| , \end{aligned} \tag{18}$$

which is equal to tracing out the coin from the derivative of the full density matrix in complete Hilbert space; i.e., tracing out the coin from Eq. (13),

$$\partial_\theta \rho_w(\theta) = \mathrm{Tr}_c[\partial_\theta \rho_\theta]. \tag{19}$$

The density matrix in position space will be in a mixed state. In the mixed state, $\rho_w^2(\theta) = \rho_w(\theta) + \rho_1(\theta)$, where $\rho_1(\theta) = \frac{\epsilon}{2}\int d\theta[\lambda \rho_w(\theta) + \rho_w(\theta)\lambda] + O(\epsilon^2)$. Here ϵ represents the fluctuation in the measure of how mixed the density matrix in position is and λ can be calculated by taking the partial derivative of $[\rho_w^2(\theta) - \rho_w(\theta)]$ with respect to θ when the fluctuation is very small. The value of λ is $[\partial_\theta \rho_w(\theta) - 1/2]$ when $[\partial_\theta \rho_w(\theta) - \rho_w(\theta)] \to 0$. Therefore the SLD is $L_\theta = 2\partial_\theta \rho_w(\theta) + \epsilon\lambda$. This implies that

$$\begin{aligned} L^2 &= 4[\partial_w(\theta)\rho_w(\theta)]^2 + 2\epsilon\{\lambda \partial_\theta \rho_w(\theta) + [\partial_\theta \rho_w(\theta)]\lambda\} + O(\epsilon^2), \\ L^2 &\approx 4[\partial_\theta \rho_w(\theta)]^2 + 2\{[L - 2\partial_\theta \rho_w(\theta)]\partial_\theta \rho_w(\theta) \\ &\quad + \partial_\theta \rho_w(\theta)[L - 2\partial_\theta \rho_w(\theta)]\}, \\ L^2 &\approx -4[\partial_\theta \rho_w(\theta)]^2 + 2[\partial_\theta \rho_w(\theta) L + L\partial_\theta \rho_w(\theta)], \end{aligned} \tag{20}$$

and therefore quantum Fisher information in the mixed state can be given by

$$\begin{aligned} H_w &= \mathrm{Tr}[\rho_w(\theta)L^2] \\ &\approx -4\mathrm{Tr}\{\rho_w(\theta)[\partial_\theta \rho_w(\theta)]^2\} + 2\mathrm{Tr}\{\rho_w(\theta) \\ &\quad \times [\partial_\theta \rho_w(\theta)L + L\partial_\theta \rho_w(\theta)]\} \\ &= 2\mathrm{Tr}\{\partial_\theta \rho_w(\theta)[L\rho_w(\theta) + \rho_w(\theta)L]\} \\ &\quad - 4\mathrm{Tr}\{\rho_w(\theta)[\partial_\theta \rho_w(\theta)]^2\} \\ &= 4\mathrm{Tr}\{[\partial_\theta \rho_w(\theta)]^2[\mathbb{I} - \rho_w(\theta)]\}. \end{aligned} \tag{21}$$

This expression for quantum Fisher information for the mixed state is obtained with an approximation that the higher powers of ϵ are very small and thus ignoring them.

Figure 3 illustrates the behavior of $H_w(\theta)$ as a function of time for different values of θ and for both bounded and unbounded DTQWs. As we have seen for the full QFI $H_f(\theta)$, also $H_w(\theta)$ increases as t^2. For t large enough (say, $t > 10$), we have $H_w(\theta) = \kappa t^2$, with the constant depending only on θ, $\kappa \equiv \kappa(\theta)$. However, some striking differences between the two cases appear after $2a$ time steps, $[-a, a]$ being the spatial interval for bounded DTQW. Those differences may be traced back to interference [58] and recurrence [59,60] in the position space. In order to illustrate this phenomenon, in Fig. 4 we show the time evolution of the so-called degree of

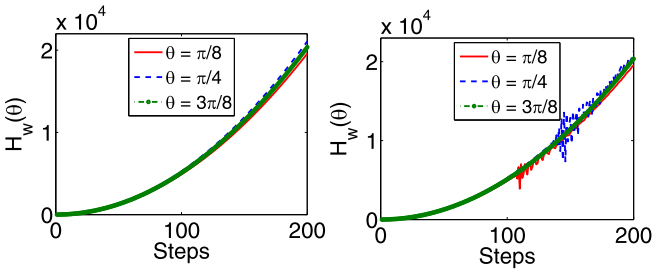

FIG. 3. The walker's position space QFI $H_w(\theta)$ as a function of time for different values of θ. Due to interference effects, we see clear differences between the walker's position space QFIs of bounded and unbounded DTQWs. The initial state of the system in both cases is $|+\rangle \otimes |0\rangle$.

interference in the position Hilbert space, i.e., the quantity

$$\mu_{x,t+1} = |\sin\theta\cos\theta\,[\rho_t^{\uparrow\downarrow}(x+1,x+1) - \rho_t^{\uparrow\downarrow}(x-1,x-1)] + \sin\theta\cos\theta[\rho_t^{\downarrow\uparrow}(x+1,x+1) - \rho_t^{\downarrow\uparrow}(x-1,x-1)]|, \quad (22)$$

defined for any site x at the time $t+1$. As it is apparent by comparing Figs. 3 and 4, the difference between $H_w(\theta)$ of bounded and unbounded DTQWs starts to appear in correspondence of the time step for which also the degrees of interference of the two cases start to differ, since the interference at a position x at time t in bounded walk is not only

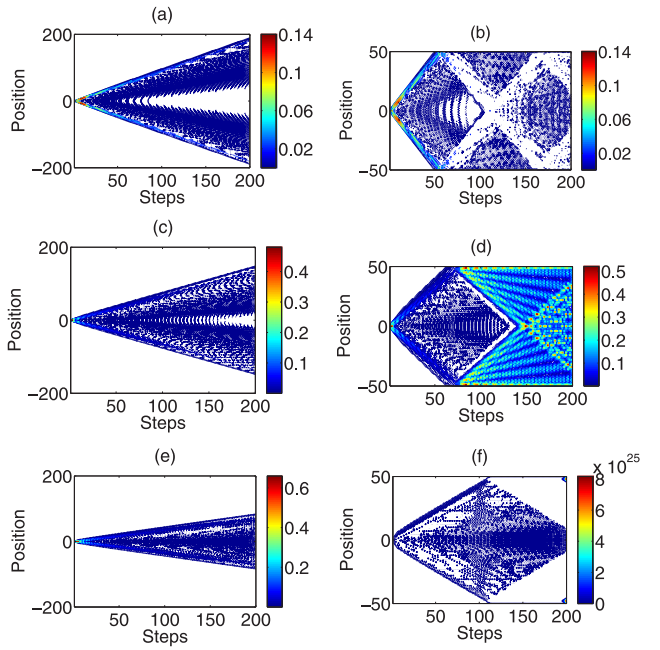

FIG. 4. Density plot of the degree of interference μ for bounded and unbounded DTQWs as a function of the time steps and the position. Panels (a) and (b) describe the behavior of μ for $\theta = \pi/8$: left panel for unbounded and right panel for bounded DTQW, respectively. Similarly, (c) and (d) correspond to the dynamics for $\theta = \pi/4$ and (e) and (f) correspond to $\theta = 3\pi/8$. The bounded walker is moving in the interval $[-50, 50]$. The initial state of the walker is $|+\rangle \otimes |x = 0\rangle$.

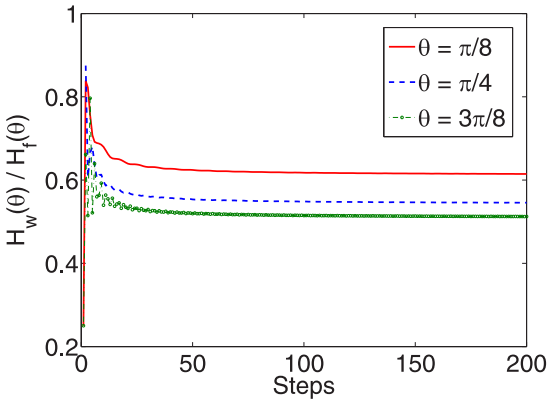

FIG. 5. Ratio of quantum Fisher information in position Hilbert space $\mathcal{H}_p$ to quantum Fisher information in complete Hilbert space $\mathcal{H} = \mathcal{H}_c \otimes \mathcal{H}_p$ for unbounded discrete-time quantum walk for 200 time steps and different values of θ. The initial state of the walker is $|+\rangle \otimes |x = 0\rangle$.

due to the neighboring sites but also due to the multiple sites. For example, in Fig. 4(b), it can be seen that for $\theta = \pi/8$ the degree of interference initially spreads over the position space with time and then starts to come back at the initial position state. After $t = 100$ time steps, interference between the reflected waves dominates, as we have seen for the QFI $H_w(\theta)$. A similar behavior (see Fig. 3 and the other panels of Fig. 4) may be observed for the other values of θ.

Figure 5 shows the ratio $H_w(\theta)/H_f(\theta)$ between the QFI of the walker's position space and the full QFI. As it is apparent from the plot, after an initial transient the ratio saturates to a constant value. More explicitly, this means that performing measurements involving the sole position degree of freedom of DTQW provides a considerable information about the coin parameter [quantified by $H_w(\theta)$], when compared to the full information that is in principle available [quantified by $H_f(\theta)$]. Notice that by measurements performed on the position degree of freedom we *do not mean* just position measurement (the performances of which are investigated in the next subsection) but rather *any* possible measurement on the walker's position Hilbert space.

Figure 6 shows the walker QFI $H_w(\theta)$ as a function of θ, for different, fixed, numbers of time steps for both unbounded and bounded DTQWs. It shows that $H_w(\theta)$ increases with θ

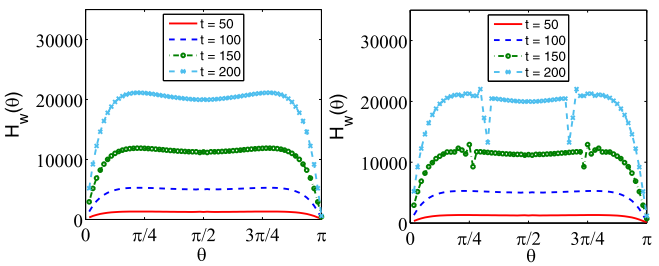

FIG. 6. The walker's position space QFI $H_w(\theta)$ as a function of θ evaluated after a different number of time steps. The differences between the QFI $H_w(\theta)$ of unbounded and bounded DTQWs is again due to interference effects in bounded DTQW. The initial state of the walker is $|+\rangle \otimes |x = 0\rangle$.

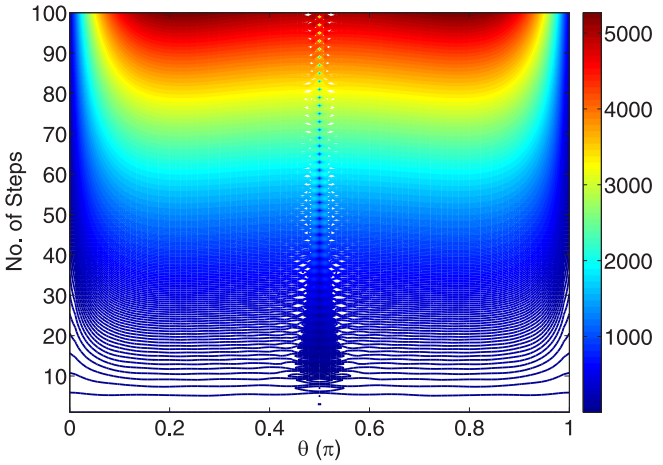

FIG. 7. QFI in position space (H_w) as a function of time steps and θ for DTQW. The initial state of the walker is $|+\rangle \otimes |x = 0\rangle$.

initially and than slowly decreases up to $\theta = \pi/2$. For θ ranging from $\theta = \pi/2$ to $\theta = \pi$ the behavior is mirrored, because of the symmetry of the quantum coin operation between. As it may be seen from the plots the behaviors of the QFI for unbounded and bounded DTQWs are very similar, except for a few more oscillations seen in the bounded case. In other words, the boundless DTQW is not particularly detrimental for its use as a probe for the coin parameter. Figure 7 shows QFI in position space H_w of DTQW in one dimension for the estimation of the coin parameter as a function of time step, and coin parameter θ is shown. This shows that for every coin parameter the QFI in position space increases with time step and therefore probability distribution measurement in position space after a larger time step will give a better estimation of coin parameter θ.

C. The FI of the walker's position measurement in discrete-time quantum walk

We now turn our attention to the performance of a specific measurement, perhaps the most natural one, i.e., the measurement on the position of the walker. The conditional probability of finding the walker at position x at time t, given that the value of the coin parameter is θ, is given by $p(x|\theta) = \mathrm{Tr}[\Pi_x \rho_w(\theta)]$ where $\{\Pi_x\} = \{|x\rangle\langle x|\}$ is the set of position projection operators and $\rho_w(\theta)$ is the density matrix of the walker, i.e., the statistical operator of Eq. (17). In other words, the position distribution of the walker is given by the diagonal elements of the density matrix $\rho_w(\theta)$ in the position representation.

Since $\rho_w(\theta)$ is carrying information on θ at any time, measuring the position provides information about the value of θ. In order to quantify this information, i.e., to quantify how much information about θ may be obtained by looking at the walker's probability distribution, one has to evaluate the position Fisher information using Eq. (8), i.e.,

$$F_x(\theta) = \sum_x \frac{[\partial_\theta p(x|\theta)]^2}{p(x|\theta)}. \tag{23}$$

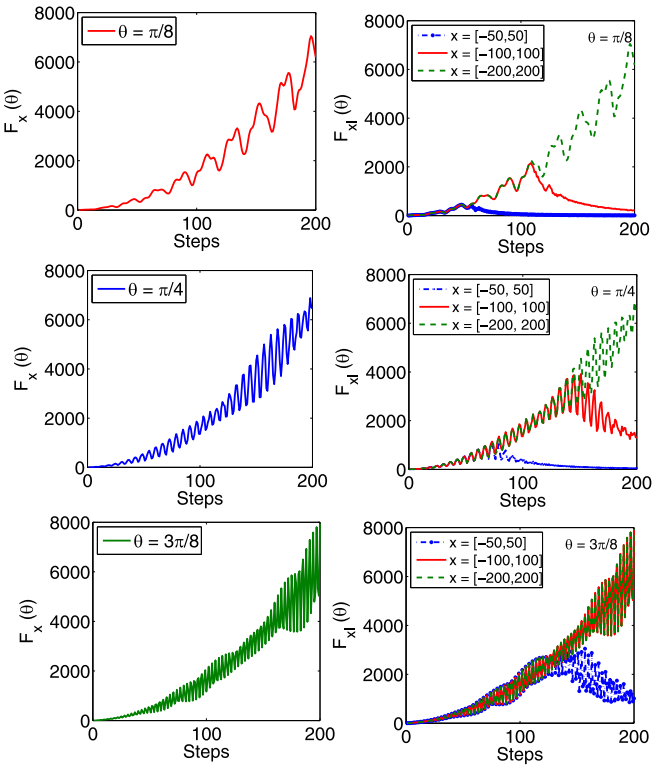

FIG. 8. The Fisher information $F_x(\theta)$ (left panels) and $F_{xl}(\theta)$ (right panels) as a function of time for unbounded DTQW and different values of θ. The initial state of the walker is $|+\rangle \otimes |x = 0\rangle$. Both sets of plots are for unbounded DTQW with $F_x(\theta)$ referring to the information extractable by a full position measurement, whereas $F_{xl}(\theta)$ quantifies the information that may be gained by measurements with limited access to the position of the walker (see text for details). The insets of the right panels are legends for the region S, accessible by the measurement.

According to the quantum Cramer-Rao bound we have $F_x(\theta) \leqslant H_w(\theta)$, and, thus, besides the absolute value of $F_x(\theta)$, we are interested in investigating how far $F_x(\theta)$ is from its bound $H_w(\theta)$; i.e., we want to compare the information extracted from position measurement to the maximum information available measuring the sole walker.

The behavior of $F_x(\theta)$ as a function of time is illustrated in the left panels of Fig. 8 for different values of θ. The FI $F_x(\theta)$ oscillates in time, with the envelope increasing as t^2, i.e., $F_x(\theta)$ shows the same scaling as $H_w(\theta)$ and $H_f(\theta)$. The right panels illustrate instead the behavior of $F_{xl}(\theta)$, which is the Fisher information of *limited* position measurement, i.e., measurement performed with detectors not able to access (i.e., to *look at*) all the possible walker's sites, but rather only to a subset S, even though the DTQW is defined on an unbounded position space. According to Eq. (8) we have

$$F_{xl}(\theta) = \sum_{x \in S} \frac{[\partial_\theta p(x|\theta)]^2}{p(x|\theta)}, \tag{24}$$

where the position distribution is still given by $p(x|\theta) = \mathrm{Tr}[\Pi_x \rho_w(\theta)]$, however with $x \in S$. In the right panels of Fig. 8 we show the behavior of $F_{xl}(\theta)$ as a function of time for different values of θ and S. The overall message is that for

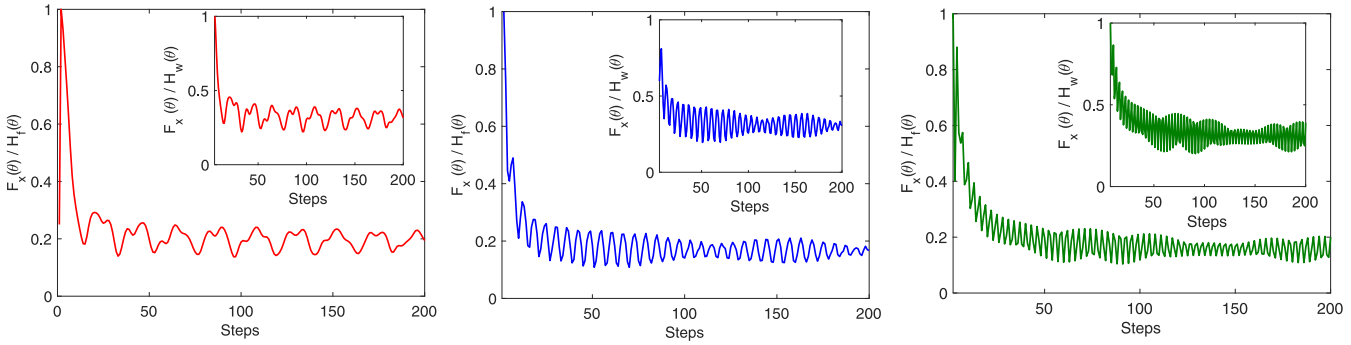

FIG. 9. The ratio $F_x(\theta)/H_f(\theta)$ between the position Fisher information and the full quantum Fisher information as a function of time and for different values of θ. The insets show the ratio $F_x(\theta)/H_w(\theta)$ between the position Fisher information and the walker's position space quantum Fisher information. All the plots refer to unbounded DTQW. The initial state of the walker is $|+\rangle \otimes |x = 0\rangle$.

short time, when the walker has negligible amplitude to be outside S, there are little differences between $F_x(\theta)$ and $F_{xl}(\theta)$, whereas for a number of time steps of the order of $|S|$ the walker is *walking beyond S* and striking differences start to appear. In particular, since in this case the measurement is not recording the full position information, the FI $F_{xl}(\theta)$ starts to decreases with time.

In order to assess the overall performances of position measurements we consider the two ratios $F_x(\theta)/H_f(\theta)$ and $F_x(\theta)/H_w(\theta)$ between the Fisher information of position measurement and the full QFI or the walker QFI, respectively. In Fig. 9 we show both the ratios as a function of time and for different values of the coin parameter θ.

D. QFI in split-step quantum walk

Split-step quantum walk is a special form of discrete-time quantum walk where a single step is split into two half steps using two coin operators C_{θ_1} and C_{θ_2} and two shift operators S_- and S_+. Split-step quantum walk has been used to simulate topological insulators [61–63], Dirac cellular automata [64], and Majorana modes and edge states [65] where the two coin operations play an important role. It has also been mapped to two period standard discrete-time quantum walks [65,66]. The evolution operator for split-step quantum walk is given by $U = S_+ C_{\theta_2} S_- C_{\theta_1}$ where

$$S_+ = \sum_x (|\uparrow\rangle\langle\uparrow| \otimes |x\rangle\langle x| + |\downarrow\rangle\langle\downarrow| \otimes |x+1\rangle\langle x|), \quad (25)$$

$$S_- = \sum_x (|\uparrow\rangle\langle\uparrow| \otimes |x-1\rangle\langle x| + |\downarrow\rangle\langle\downarrow| \otimes |x\rangle\langle x|), \quad (26)$$

and the coin operator is given by

$$C_{\theta_j} = \begin{pmatrix} \cos\theta_j & -i\sin\theta_j \\ -i\sin\theta_j & \cos\theta_j \end{pmatrix} \otimes \sum_x |x\rangle\langle x|, \quad (27)$$

where $j = 1, 2$.

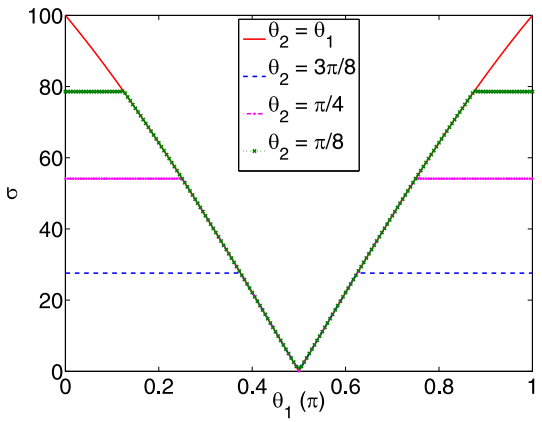

FIG. 10. The standard deviation for split-step quantum walk as function of θ_1 for different values of θ_2 after 100 steps of walk. Standard deviation is always bounded by the larger θ parameter. Therefore it only gives information of the evolution parameter with the higher value. The initial state of the walker is $|+\rangle \otimes |x = 0\rangle$.

Estimation of both the parameters θ_1 and θ_2 using standard deviation is not possible, as has already been studied in the past [66]. In Fig. 10 we show the standard deviation of unbounded split-step quantum walk after 100 steps of walk as a function of θ_1 when θ_2 is fixed. We can note that the standard deviation is always bounded by the larger of the two parameters θ_1 and θ_2. But using the quantum Fisher information for both the parameters individually in position space, each of the parameters can be estimated. It can be seen in Fig. 11 that QFI in position space with respect to θ_2 for different values of θ_1 shows that $H_w(\theta_2)$ is minimum for $\theta_2 = \theta_1$ and QFI in position space with respect to θ_1 for different values θ_2 shows that $H_w(\theta_1)$ is maximum for $\theta_2 = \theta_1$. Since QFI in position space is a measure of how precisely one can estimate the evolution parameters on measurement of probability distribution in position space, Fig. 11 shows that, given the value of parameter θ_1, θ_2 can be estimated more precisely when $\theta_2 \neq \theta_1$ as $H_w(\theta_2)$ is minimum when $\theta_2 = \theta_1$. Similarly $H_w(\theta_1)$ shows that the amount of information of θ_1 is maximum when $\theta_1 = \theta_2$ on measurement of the probability distribution. This estimation is not possible by just measuring the standard deviation in the split-step quantum walk.

IV. CONCLUSION

In this paper, we have investigated probing techniques for the coin parameter θ of discrete-time quantum walk, which, in turn, plays a crucial role in providing quadratic speed-up over its classical counterpart. In particular, we have addressed the ultimate bounds to precision, as obtained by performing the

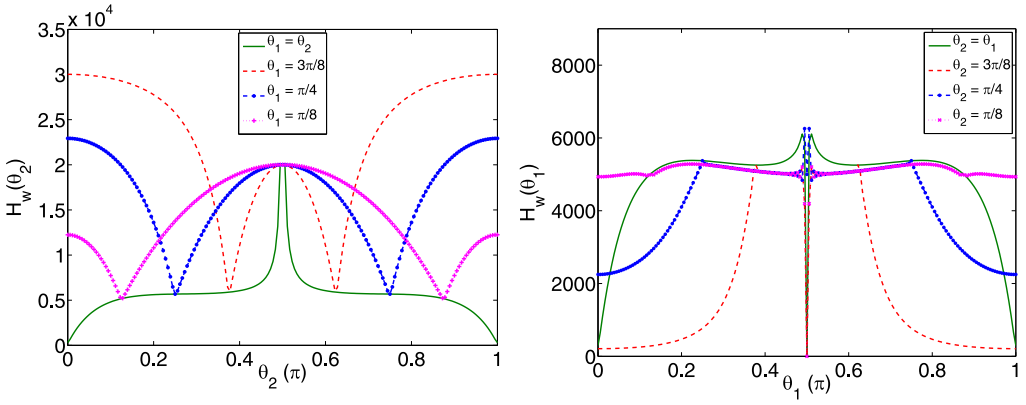

FIG. 11. Quantum Fisher information in position space with respect to the evolution parameters θ_2 (left) and θ_1 (right) when other parameters are fixed. Having clearly distinct plots for both parameters after 100 time steps helps us to uniquely probe both parameters independently. The initial state of the walker is $|+\rangle \otimes |x = 0\rangle$.

optimal measurement on the particle. Our approach is based on the fact that the walker's coin space entangles with the position space after the very first step of the evolution, such that we may estimate the value of the coin parameter θ by performing measurements on the sole position space of the walker.

We have found that the QFI of the walker's position space $H_w(\theta)$ increases with θ and with time, which, in turn, may be seen as a metrological resource. We also find a difference in the QFI of *bounded* and *unbounded* DTQWs and provide an interpretation of the different behaviors in terms of interference in the position space. We have also compared $H_w(\theta)$ to the full QFI $H_f(\theta)$, i.e., the QFI of the walker's position plus coin state, and find that their ratio is dependent on θ, but saturates to a constant value, meaning that the walker may probe its coin parameter quite faithfully. Finally, we have found that if one has access to a limited region in position space the QFI depends only on the sites with nonzero probability of finding a particle. Therefore, when one has access to an incomplete position space, after some steps (equal to half of the number of accessible sites) we see a decrease of QFI.

Though standard deviation and group velocity help us to estimate one-parameter QW, they fail to provide a reasonable estimation in the case of bounded QW and two-parameter split-step QW. We can overcome this using QFI. Our results show that estimation of the coin parameter in DTQW is possible with realistic detection schemes and pave the way for further developments in the field of quantum probing for complex networks.

ACKNOWLEDGMENTS

C.M.C. would like to thank the Department of Science and Technology, Government of India for the Ramanujan Fellowship Grant No. SB/S2/RJN-192/2014. This work has been supported by SERB through Project No. VJR/2017/000011. M.G.A.P. is a member of GNFM-INdAM.

[1] G. V. Ryazanov, The Feynman path integral for the Dirac equation, JETP **6**, 1107 (1958).
[2] R. P. Feynman, Quantum mechanical computers, Found. Phys. **16**, 507 (1986).
[3] K. R. Parthasarathy, The passage from random walk to diffusion in quantum probability, J. Appl. Probab. **25**, 151 (1988).
[4] Y. Aharonov, L. Davidovich, and N. Zagury, Quantum random walks, Phys. Rev. A **48**, 1687 (1993).
[5] D. A. Meyer, From quantum cellular automata to quantum lattice gases, J. Stat. Phys. **85**, 551 (1996).
[6] J. Kempe, Quantum random walks: An introductory overview, Contemp. Phys. **44**, 307 (2003).
[7] S. E. Venegas-Andraca, Quantum walks: A comprehensive review, Quant. Info. Proc. **11**, 1015 (2012).
[8] A. M. Childs, R. Cleve, E. Deotto, E. Farhi, S. Gutmann, and D. A. Spielman, Exponential algorithmic speedup by a quantum walk, in *Proceedings of the Thirty-Fifth Annual ACM Symposium on Theory of Computing* (ACM, New York, 2003), pp. 59–68.
[9] A. M. Childs and J. Goldstone, Spatial search by quantum walk, Phys. Rev. A **70**, 022314 (2004).
[10] A. Ambainis, Quantum walk algorithm for element distinctness, SIAM J. Comput. **37**, 210 (2007).
[11] F. Magniez, M. Santha, and M. Szegedy, Quantum algorithms for the triangle problem, SIAM J. Comput. **37**, 413 (2007).
[12] H. Buhrman and R. Špalek, Quantum verification of matrix products, in *Proceedings of the Seventeenth Annual ACM-SIAM Symposium on Discrete Algorithms* (Society for Industrial and Applied Mathematics, Philadelphia, PA, 2006), pp. 880–889.
[13] E. Farhi, J. Goldstone, and S. Gutmann, A quantum algorithm for the Hamiltonian NAND tree, Th. Comput. **4**, 169 (2008).
[14] N. Konno, Quantum walks, in *Quantum Potential Theory* (Springer, New York, 2008), pp. 309–452.
[15] G. S. Engel, T. R. Calhoun, E. L. Read, T.-K. Ahn, T. Mančal, Y.-C. Cheng, R. E. Blankenship, and G. R. Fleming, Evidence for wavelike energy transfer through quantum coherence in photosynthetic systems, Nature (London) **446**, 782 (2007).

[16] M. Mohseni, P. Rebentrost, S. Lloyd, and A. Aspuru-Guzik, Environment-assisted quantum walks in photosynthetic energy transfer, J. Chem. Phys. **129**, 174106 (2008).

[17] C. M. Chandrashekar and T. Busch, Quantum percolation and transition point of a directed discrete-time quantum walk, Sci. Rep. **4**, 6583 (2014).

[18] B. Kollár, T. Kiss, J. Novotný, and I. Jex, Asymptotic Dynamics of Coined Quantum Walks on Percolation Graphs, Phys. Rev. Lett. **108**, 230505 (2012).

[19] B. L. Douglas and J. B. Wang, A classical approach to the graph isomorphism problem using quantum walks, J. Phys. A **41**, 075303 (2008).

[20] A. M. Childs, Universal Computation by Quantum Walk, Phys. Rev. Lett. **102**, 180501 (2009).

[21] A. Joye, Dynamical localization for d-dimensional random quantum walks, Quant. Info. Proc. **11**, 1251 (2012).

[22] C. M. Chandrashekar, Disorder induced localization and enhancement of entanglement in one-and two-dimensional quantum walks, arXiv:1212.5984.

[23] C. M. Chandrashekar and T. Busch, Localized quantum walks as secured quantum memory, Europhys. Lett. **110**, 10005 (2015).

[24] H. Obuse and N. Kawakami, Topological phases and delocalization of quantum walks in random environments, Phys. Rev. B **84**, 195139 (2011).

[25] T. Kitagawa, M. S. Rudner, E. Berg, and E. Demler, Exploring topological phases with quantum walks, Phys. Rev. A **82**, 033429 (2010).

[26] A. Mallick, S. Mandal, and C. M. Chandrashekar, Neutrino oscillations in discrete-time quantum walk framework, Eur. Phys. J. C **77**, 85 (2017).

[27] G. Di Molfetta and A. Pérez, Quantum walks as simulators of neutrino oscillations in a vacuum and matter, New J. Phys. **18**, 103038 (2016).

[28] F. W. Strauch, Relativistic quantum walks, Phys. Rev. A **73**, 054302 (2006).

[29] C. M. Chandrashekar, S. Banerjee, and R. Srikanth, Relationship between quantum walks and relativistic quantum mechanics, Phys. Rev. A **81**, 062340 (2010).

[30] C. M. Chandrashekar, Two-component Dirac-like Hamiltonian for generating quantum walk on one-, two-, and three-dimensional lattices, Sci. Rep. **3**, 2829 (2013).

[31] G. Di Molfetta, M. Brachet, and F. Debbasch, Quantum walks as massless Dirac fermions in curved space-time, Phys. Rev. A **88**, 042301 (2013).

[32] G. Di Molfetta, M. Brachet, and F. Debbasch, Quantum walks in artificial electric and gravitational fields, Physica A **397**, 157 (2014).

[33] P. Arrighi, S. Facchini, and M. Forets, Quantum walking in curved spacetime, Quant. Info. Proc. **15**, 3467 (2016).

[34] A. Pérez, Asymptotic properties of the Dirac quantum cellular automaton, Phys. Rev. A **93**, 012328 (2016).

[35] C. A. Ryan, M. Laforest, J.-C. Boileau, and R. Laflamme, Experimental implementation of a discrete-time quantum random walk on an NMR quantum-information processor, Phys. Rev. A **72**, 062317 (2005).

[36] A. Schreiber, K. N. Cassemiro, V. Potoček, A. Gábris, P. J. Mosley, E. Andersson, I. Jex, and C. M. Silberhorn, Photons Walking the Line: A Quantum Walk with Adjustable Coin Operations, Phys. Rev. Lett. **104**, 050502 (2010).

[37] M. A. Broome, A. Fedrizzi, B. P. Lanyon, I. Kassal, A. Aspuru-Guzik, and A. G. White, Discrete Single-Photon Quantum Walks with Tunable Decoherence, Phys. Rev. Lett. **104**, 153602 (2010).

[38] A. Peruzzo, M. Lobino, J. C. Matthews, N. Matsuda, A. Politi, K. Poulios, X.-Q. Zhou, Y. Lahini, N. Ismail, K. Wörhoff *et al.*, Quantum walks of correlated photons, Science **329**, 1500 (2010).

[39] H. B. Perets, Y. Lahini, F. Pozzi, M. Sorel, R. Morandotti, and Y. Silberberg, Realization of Quantum Walks with Negligible Decoherence in Waveguide Lattices, Phys. Rev. Lett. **100**, 170506 (2008).

[40] M. Karski, L. Förster, J.-M. Choi, A. Steffen, W. Alt, D. Meschede, and A. Widera, Quantum walk in position space with single optically trapped atoms, Science **325**, 174 (2009).

[41] H. Schmitz, R. Matjeschk, C. Schneider, J. Glueckert, M. Enderlein, T. Huber, and T. Schaetz, Quantum Walk of a Trapped Ion in Phase Space, Phys. Rev. Lett. **103**, 090504 (2009).

[42] F. Zähringer, G. Kirchmair, R. Gerritsma, E. Solano, R. Blatt, and C. F. Roos, Realization of a Quantum Walk with One and Two Trapped Ions, Phys. Rev. Lett. **104**, 100503 (2010).

[43] C. M. Chandrashekar, R. Srikanth, and R. Laflamme, Optimizing the discrete time quantum walk using a SU(2) coin, Phys. Rev. A **77**, 032326 (2008).

[44] A. Ahlbrecht, H. Vogts, A. H. Werner, and R. F. Werner, Asymptotic evolution of quantum walks with random coin, J. Math. Phys. **52**, 042201 (2011).

[45] A. Smirne, S. Cialdi, G. Anelli, M. G. A. Paris, and B. Vacchini, Quantum probes to experimentally assess correlations in a composite system, Phys. Rev. A **88**, 012108 (2013).

[46] C. Benedetti, F. Buscemi, P. Bordone, and M. G. A. Paris, Quantum probes for the spectral properties of a classical environment, Phys. Rev. A **89**, 032114 (2014).

[47] M. G. Paris, Quantum probes for fractional gaussian processes, Physica A **413**, 256 (2014).

[48] C. Benedetti and M. G. Paris, Characterization of classical Gaussian processes using quantum probes, Phys. Lett. A **378**, 2495 (2014).

[49] M. A. Rossi and M. G. A. Paris, Entangled quantum probes for dynamical environmental noise, Phys. Rev. A **92**, 010302(R) (2015).

[50] D. Tamascelli, C. Benedetti, S. Olivares, and M. G. A. Paris, Characterization of qubit chains by Feynman probes, Phys. Rev. A **94**, 042129 (2016).

[51] L. Seveso and M. G. A. Paris, Can quantum probes satisfy the weak equivalence principle? Ann. Phys. **380**, 213 (2017).

[52] M. Bina, F. Grasselli, and M. G. A. Paris, Continuous-variable quantum probes for structured environments, Phys. Rev. A **97**, 012125 (2018).

[53] C. Benedetti, F. S. Sehdaran, M. H. Zandi, and M. G. A. Paris, Quantum probes for the cutoff frequency of ohmic environments, Phys. Rev. A **97**, 012126 (2018).

[54] F. Troiani and M. G. A. Paris, Universal Quantum Magnetometry with Spin States at Equilibrium, Phys. Rev. Lett. **120**, 260503 (2018).

[55] A. Beggi, L. Razzoli, P. Bordone, and M. G. A. Paris, Probing the sign of the Hubbard interaction by two-particle quantum walks, Phys. Rev. A **97**, 013610 (2018).

[56] I. Pizio, S. Singh, C. M. Chandrashekar, and M. G. A. Paris, Quantum probes for quantum wells, arXiv:1808.06757.

[57] M. G. A. Paris, Quantum estimation for quantum technology, Int. J. Quantum. Inform. **7**, 125 (2009).

[58] S. Singh and C. M. Chandrashekar, Interference in localized quantum walk, arXiv:1711.06217.

[59] M. Štefaňák, I. Jex, and T. Kiss, Recurrence and Pólya number of Quantum Walks, Phys. Rev. Lett. **100**, 020501 (2008).

[60] C. M. Chandrashekar, Fractional recurrence in discrete-time quantum walk, Open Phys. **8**, 979 (2010).

[61] B. Tarasinski, J. K. Asbóth, and J. P. Dahlhaus, Scattering theory of topological phases in discrete-time quantum walks, Phys. Rev. A **89**, 042327 (2014).

[62] J. K. Asbóth, Symmetries, topological phases, and bound states in the one-dimensional quantum walk, Phys. Rev. B **86**, 195414 (2012).

[63] T. Kitagawa, M. A. Broome, A. Fedrizzi, M. S. Rudner, E. Berg, I. Kassal, A. Aspuru-Guzik, E. Demler, and A. G. White, Observation of topologically protected bound states in photonic quantum walks, Nat. Commun. **3**, 882 (2012).

[64] A. Mallick and C. M. Chandrashekar, Dirac cellular automaton from split-step quantum walk, Sci. Rep. **6**, 25779 (2016).

[65] W.-W. Zhang, S. K. Goyal, C. M. Simon, and B. C. Sanders, Decomposition of split-step quantum walks for simulating Majorana modes and edge states, Phys. Rev. A **95**, 052351 (2017).

[66] N. P. Kumar, R. Balu, R. Laflamme, and C. M. Chandrashekar, Bounds on the dynamics of periodic quantum walks and emergence of the gapless and gapped Dirac equation, Phys. Rev. A **97**, 012116 (2018).